

# Datapath Synthesis for Overclocking: Online Arithmetic for Latency-Accuracy Trade-offs

Authors removed for blind review

## ABSTRACT

In this paper we take a fresh look at Online Arithmetic, originally proposed for digit-serial operation, and synthesize unrolled digit-parallel online operators to allow for graceful degradation under overclocking. We quantify the impact of timing violation on key arithmetic primitives, and show that substantial performance benefits can be obtained in comparison to binary arithmetic. Since timing errors are generated in least significant digits with online arithmetic, less impact is caused than conventional implementations. Using analytical models and empirical FPGA results, we demonstrate an error reduction over 89% and an improvement in SNR of over 20dB for the same clock rate.

## Categories and Subject Descriptors

B.2.4 [Arithmetic and Logic Structures]: High-Speed Arithmetic—*Algorithms, Cost/performance*

## General Terms

Design, Performance, Reliability

## Keywords

Online Arithmetic, Overclocking, Imprecise Design

## 1. INTRODUCTION

Circuit performance has increased tremendously over the past decades with the continuous scaling of CMOS technology such that they occupy less area and operate faster. Typically static-timing analysis incorporates safety margins for timing closure. However, continuing with this approach could become very expensive in the short term future. As circuit dimensions scale down, it is increasingly difficult to maintain low relative manufacturing-variation. Because timing margins in static-analysis tools increase with process variability, designing for worst-case delay in circuits becomes increasingly costly as relative process variation rises.

While datapath can be pipelined to boost clock frequency, this does not reduce overall computational latency. In em-

bedded applications, which often have strict latency requirements, or in any datapath containing feedback, where C-slow retiming is inappropriate, pipelining does not help meet performance targets. To overcome these problems, a large volume of studies have demonstrated that relaxing the absolute datapath-accuracy requirements can provide the freedom to create designs with better performance or energy efficiency [1, 7, 9, 10].

However, we notice that most research in this area focuses on standard binary arithmetic [7, 9, 10], which potentially suffers from large magnitude of timing errors. This is because, in standard arithmetic operators such as ripple-carry adders, the most significant digit (MSD) is updated *last* due to carry propagation, so timing violation initially affects the MSD of the result. In this paper, for the first time we attempt to solve this problem by adopting an alternative form of MSD-first arithmetic known as online arithmetic. We evaluate the probabilistic behavior of basic arithmetic primitives with different types of arithmetic when operating beyond the deterministic clocking region. We suggest that in comparison to conventional arithmetic, operators employing this arithmetic are less sensitive to overclocking, because timing errors only affect the least significant digits. To support this hypothesis, we propose probabilistic models of error for an online multiplier. We back up the models with experimental results from an image processing application. We demonstrate that our novel design methodology can lead to substantial performance benefits compared to the design method using conventional arithmetic. A summary of the main contributions of this paper are as follows:

- to our knowledge, the first “overclocking friendly” computer arithmetic,
- probabilistic models of overclocking errors for a digit-parallel online multiplier,
- analytical and empirical results which demonstrate that the impact of timing violations is ameliorated with online arithmetic and that large performance benefits can be achieved.

## 2. BACKGROUND

### 2.1 Online Arithmetic

In conventional arithmetic, the computation results are generated either from the least significant digit (LSD), e.g. addition and multiplication, or from the MSD, e.g. division and square root. This inconsistency in computing directions

can result in large latency when propagating data among different operations. To tackle this problem, online arithmetic has been proposed and studied over the past few decades [4, 13, 11]. Both the inputs and outputs are processed in a MSD-first manner using online arithmetic, enabling parallelism among multiple operations. Therefore the overall latency can be greatly reduced.

Originally online arithmetic was designed for digit-serial operation. In order to generate the first output digit,  $\delta$  digits of inputs are required, as illustrated in Figure 1.  $\delta$  is known as the online delay, which is a constant, independent of the precision in a given operation. For ease of discussion, the input to our circuit is normalized to a fixed point number in the range  $(-1, 1)$ . Based on this premise, the online representations of  $N$ -digit operands and result at iteration  $j$  are given by (1) for  $j \in [-\delta, N-1]$  and  $r$  denotes the radix [5].

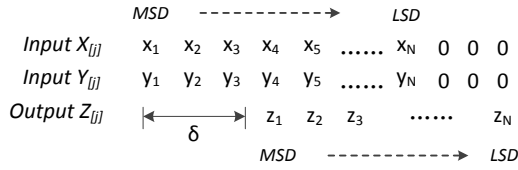


Figure 1: Dataflow in digit-serial Online Arithmetic.

$$X_{[j]} = \sum_{i=1}^{j+\delta} x_i r^{-i}, \quad Y_{[j]} = \sum_{i=1}^{j+\delta} y_i r^{-i}, \quad Z_{[j]} = \sum_{i=1}^j z_i r^{-i} \quad (1)$$

MSD-first operation in online arithmetic is possible because they adopt a redundant number system [2], in which each digit is represented with a redundant digit set  $\{-a, \dots, -1, 0, 1, \dots, a\}$ , where  $a \in [r/2, r-1]$ . Due to the redundancy, the MSDs of the result can be estimated only based on partial information of the inputs and then the value of the number can be revised by the following digits.

## 2.2 Radix-2 Digit-parallel Online Adder

Adders serve as a critical building block for arithmetic operations. To perform digit-parallel online addition, a redundant adder can be directly utilized. The adder structure diagram is shown in Figure 2. A major advantage with the redundant number system over the standard ripple-carry based arithmetic is that the propagation of carry is eliminated, resulting in a precision-independent computation time for addition. As seen in Figure 2, the computation delay of this adder is only 2 full adder (FA) delays for any operand word-length, with the cost of one extra FA for each digit of operands. This makes online adder suitable for building up more complex arithmetic operators such as multipliers to accelerate the sum of partial products [8, 12].

## 2.3 Radix-2 Digit-parallel Online Multiplier

Multiplication is another key primitive of arithmetic operations. Typically the online multiplication is performed in a recursive digit-serial manner, as illustrated in Algorithm 1 where both inputs and outputs are  $N$ -digit number as represented in (1). For a given iteration  $j$ , the product digit  $z_j$  is generated through a selection function  $sel()$ . For the radix  $r$  and a chosen digit set, there exists an appropriate selection method and a value of  $\delta$  which ensure convergence. As radix-2 is used most commonly in computer arithmetic,

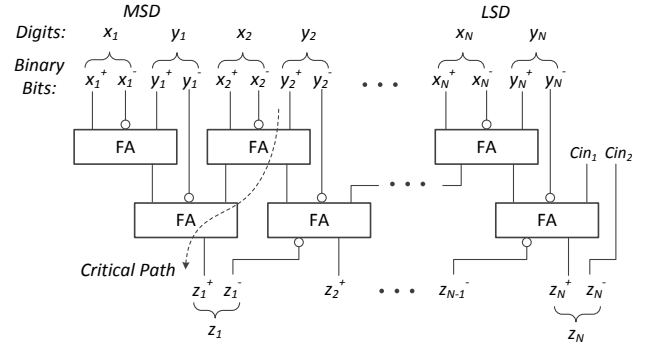


Figure 2: An  $N$ -digit binary digit-parallel online adder.

### Algorithm 1 Online Multiplication

**Initialization:**  $X_{[-\delta]} = Y_{[-\delta]} = P_{[-\delta]} = 0$

**Recurrence:** *for*  $j = -\delta, -\delta+1, \dots, N-1$  *do*

$$\begin{aligned} H_{[j]} &= r^{-\delta} (x_{j+\delta+1} \cdot Y_{[j+1]} + y_{j+\delta+1} \cdot X_{[j]}) \\ W_{[j]} &= P_{[j]} + H_{[j]} \\ z_j &= sel(W_{[j]}) \\ P_{[j+1]} &= r(W_{[j]} - z_j) \end{aligned} \quad (2)$$

we keep  $r = 2$  throughout this paper with the corresponding redundant digit set  $\{\bar{1}, 0, 1\}$ . In this case we have  $\delta = 3$ , and  $sel()$  is given by (3) [6], from which it can be seen that the decision is made only based on 1 integer bit and 1 fractional bit of  $W_{[j]}$ .

$$sel(W_{[j]}) = \begin{cases} 1 & \text{if } W_{[j]} \geq \frac{1}{2} \\ 0 & \text{if } -\frac{1}{2} \leq W_{[j]} < \frac{1}{2} \\ \bar{1} & \text{if } W_{[j]} < -\frac{1}{2} \end{cases} \quad (3)$$

Algorithm 1 can be synthesized into a unrolled digit parallel structure as shown in Figure 3(a). In an  $N$ -digit online multiplier (OM), there are totally  $N + \delta$  stages, of which the online inputs are generated from the appending logic according to (1). In each stage, an online adder is used as shown in Figure 3(b). The SDVM module performs the signed-digit vector multiplication. When  $r = 2$  and the digit set  $\{\bar{1}, 0, 1\}$  is used, the implementation of SDVM is straight forward, because for instance the output of  $(y_{j+\delta+1} \cdot X_{[j]})$  is 0,  $X_{[j]}$  or  $-X_{[j]}$  when  $y$  is equal to 0, 1 and  $-1$  respectively.

Instead of duplicating the digit-serial implementation  $N + \delta$  times, each stage in the digit-parallel architecture can be optimized for area reduction. For instance, the SDVM modules and the appending logic are not required in the last  $\delta$  stages because the inputs are 0. This leads to a smaller online adder in these stages. Similarly for the first  $\delta$  stages the selection logic can be removed, as the first digit of the result is generated at stage 0 ( $S_0$ ).

## 3. PROBABILISTIC MODEL OF OVERCLOCKING ERROR

As it is unlikely that timing violation happens in the online adder, in this Section we model the overclocking error in the radix-2 OM. From Figure 3 we observe two types of delay chains. One is caused by generation and propagation of  $P_{[j]}$  among different stages. The other is the generation of online

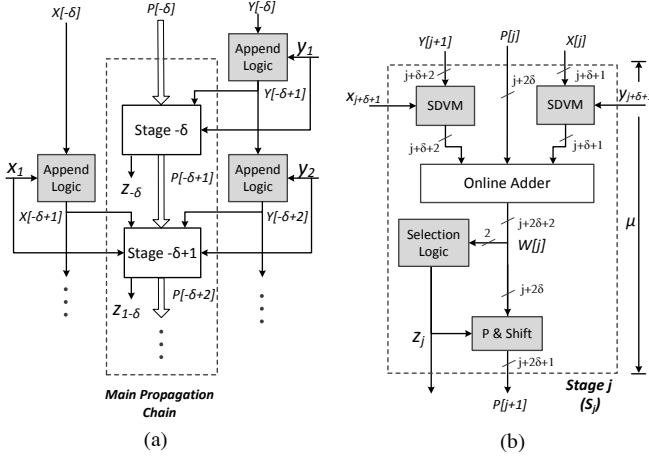


**Figure 3: (a) Synthesis of Algorithm 1 into a digit-parallel online multiplier (b) Structure of one stage, in which the maximum digit widths of signals are labeled.**

inputs  $X[j]$  and  $Y[j]$  from the appending logic. Since the appending logic is basically wires and simple combinational logic [3], the overall latency will eventually be determined by the delay of the  $P[j]$  path, especially with increasing operand word-lengths. As such, we initially model the delay of each stage within an OM to be a constant value  $\mu$ , as shown in Figure 3(b). We also assume that the generation of online inputs costs no delay.

Let  $\mu_{OM}$  denote the worst-case delay of an OM. It follows that if the clock period  $T_S$  is greater than  $\mu_{OM}$ , correct results will be sampled. If, however, faster-than-rated sampling frequencies are applied such that  $T_S < \mu_{OM}$ , timing violations might happen and intermediate results will be sampled, potentially generating errors. For a given  $T_S$ , the maximum length of error-free propagation is described by (4) where  $f_s$  denotes the sampling frequency. We always ensure that the first digit of the product will be generated correctly, i.e.  $b > \delta$ .

$$b := \left\lceil \frac{T_S}{\mu} \right\rceil = \left\lceil \frac{1}{\mu \cdot f_s} \right\rceil \quad (4)$$

We now determine when this timing constraint is not met and the size of error in this case. We assume in the models that every digit of input signal to our circuit is uniformly and independently generated with the digit set  $\{1, 0, 1\}$ . However this assumption will be relaxed in Section 4 where real input data are used.

### 3.1 Probability of Timing Violations

For an  $N$ -digit OM, let a propagation chain be generated at stage  $S_\tau$  with the length of  $d(\tau)$  digits, then the stage number  $\tau$  is bounded by (5). The presence of timing violation requires  $d(\tau) > b$ . Besides, the chain cannot propagate over  $S_{N-1}$ . Thus the bound of parameter  $d(\tau)$  is given by (6).

$$-\delta \leq \tau \leq N - 1 - b = \tau_{max} \quad (5)$$

$$b < d(\tau) \leq N - 1 - \tau \quad (6)$$

However, the actual length of a “carry” chain is dependent upon input patterns. We then examine the relationship between  $d(\tau)$  and the inputs that corresponds to the genera-

tion, propagation and annihilation of this carry chain. Let the specific input pattern of stage  $S_\tau$  be represented by  $C(\tau)$ , which can be classified into four types, as listed in (7). Under the assumption that all digits are mutually independent and uniformly distributed, the probability of  $C_1 \sim C_4$  equal to 1/9, 4/9, 2/9 and 2/9 respectively.

$$C(\tau) = \begin{cases} \text{Case 1 } (C_1) : & x_{\tau+\delta+1} = 0, y_{\tau+\delta+1} = 0 \\ \text{Case 2 } (C_2) : & x_{\tau+\delta+1} \neq 0, y_{\tau+\delta+1} \neq 0 \\ \text{Case 3 } (C_3) : & x_{\tau+\delta+1} \neq 0, y_{\tau+\delta+1} = 0 \\ \text{Case 4 } (C_4) : & x_{\tau+\delta+1} = 0, y_{\tau+\delta+1} \neq 0 \end{cases} \quad (7)$$

The classification is based on whether a digit is zero, as all internal signals are reset to zero initially. Under this premise, (2) can be modified to give (8) for  $\tau > -\delta$ . If  $C(\tau) = C_1$ , no chain will be generated at  $S_\tau$  because  $P_{[\tau+1]} = 0$ .

$$\begin{aligned} P_{[\tau+1]} &= r \cdot W_{[\tau]} \\ &= r^{-\delta+1} (x_{\tau+\delta+1} Y_{[\tau+1]} + y_{\tau+\delta+1} X_{[\tau]}) \end{aligned} \quad (8)$$

In other cases,  $P_{[\tau+1]} \neq 0$  and a new chain will be generated at  $S_\tau$ . We denote the number of the leading non-zero digits of  $P_{[\tau+1]}$  to be  $D$ . When  $P_{[\tau+1]}$  propagates to the next stage, from (2) we notice that  $D = D - 1$ , because of the 1-digit shifting when computing  $P_{[\tau+1]} = r(W_{[\tau]} - z_\tau)$ . This process is independent of inputs. Finally, this chain will be annihilated when  $D = 1$ . In summary, chain length  $d(\tau)$  is related to the value of  $D$ , which we consider separately for  $C(\tau) = C_2, C_3$  and  $C_4$ .

If  $C(\tau) = C_2$ ,  $D$  equals to the maximum word-length of  $P_{[\tau+1]}$  as shown in Figure 3(b), i.e.  $D = \tau + 2\delta + 1$ . Combining  $D$  and (6) gives the maximum chain length in (9).

$$\begin{aligned} d(\tau)_{max} &= \text{Min}(D, N - 1 - \tau) \\ &= \text{Min}(\tau + 2\delta + 1, N - 1 - \tau) \end{aligned} \quad (9)$$

For  $C_3$  and  $C_4$ , the carry generation, propagation and annihilation behavior of both cases are identical. Hence we only discuss  $C(\tau) = C_3$ . In this situation, (8) is modified to give (10). We have  $Y_{[\tau+1]} = Y_{[\tau]}$  as  $y_{\tau+\delta+1} = 0$ . Thus  $D$  only depends on the number of the leading non-zero digits of  $Y_{[\tau]}$ .

$$P_{[\tau+1]} = r^{-\delta+1} (x_{\tau+\delta+1} Y_{[\tau+1]}) = r^{-\delta+1} (x_{\tau+\delta+1} Y_{[\tau]}) \quad (10)$$

For the first stage where  $\tau = -\delta$ , substituting this into (10) yields  $P_{[-\delta+1]} = r^{-\delta+1} (x_1 y_1)$ . Therefore  $d(-\delta) = d(-\delta)_{max}$  as given in (9), and it is obtained only when  $C(-\delta) = C_2$ , otherwise  $d(-\delta) = 0$ .

If the carry chain is generated from other stages where  $\tau > -\delta$ ,  $D$  and  $d(\tau)$  can be determined from 2 possible situations for  $\tau' = \tau - 1$  as stated below:

- If  $y_{\tau'+\delta+1} \neq 0$ ,  $D$  equals to the maximum word-length of  $Y_{[\tau'+1]}$ . Thus we have  $d(\tau) = d(\tau')_{max} - 1$ .
- If  $y_{\tau'+\delta+1} = 0$ ,  $Y_{[\tau']} = Y_{[\tau'-1]}$ . This is a recursive process and these two judgements will be performed again for  $\tau'' = \tau' - 1$ . It terminates when the first judgement is satisfied or the first stage is reached.

The entire process can be summarized into Algorithm 2, which examines all possible stages that timing violations may occur, and all possible input patterns for each stage. This algorithm returns  $Pr(T_S)$ , which denotes the probability that timing violations happen in an  $N$ -digit online multiplier as a function of  $T_S$ . In this algorithm,  $b$  and  $\tau_{max}$

are obtained from (4) and (5). The probability of the input pattern for stage  $i$  is denoted by  $Pr(C(i))$ , which can be determined through (7).

---

**Algorithm 2** Probability of Timing Violations

---

```

1:  $Pr(T_S) \leftarrow 0$ 
2: for all stages  $\tau \in \{-\delta, -\delta + 1, \dots, \tau_{max}\}$  and all input
   cases  $C(\tau) \in \{C_1, \dots, C_4\}$  do
3:   Determine  $d(\tau)$  based on  $C(\tau)$ 
4:   if  $d(\tau) > b$  then
5:      $Pr(T_S) \leftarrow Pr(T_S) + \prod_{i=-\delta}^{\tau} Pr(C(i))$ 
6:   end if
7: end for
8: return  $Pr(T_S)$ 

```

---

### 3.2 Magnitude of Overclocking Error

In the presence of timing violation, multiple chains might not be correctly propagated, resulting in overclocking errors generated from LSDs. We now locate the first output digit  $z_\lambda$  that contains error. For a given  $T_S$  and a minimum value of  $\tau$  such that  $d(\tau)_{max} > b$ , we have  $\lambda = \tau + d(\tau)_{max} + 1$  for chain annihilation. As such, the magnitude of overclocking error can be expressed by (11), where  $z_i$  and  $z_i'$  denote the correct value and the actual value of the output digit of  $S_i$ , separately, and  $\varepsilon_i \in \{\pm 2^{-i}, \pm 2^{-i+1}\}$  since  $z$  is represented using digit set  $\{\bar{1}, 0, 1\}$ .

$$|\varepsilon| = \left| \sum_{i=\lambda}^N 2^{-i} (z_i - z_i') \right| = \left| \sum_{i=\lambda}^N \varepsilon_i \right| \quad (11)$$

However, the changing of the product digits may not result in a different number as it is represented in a redundant form. For instance, the two's complement number 0.111 can be represented in the online form as 0.10 $\bar{1}$ , 0.0 $\bar{1}$ 1 and 0.111. This will lead to a smaller error magnitude in practice. In contrast, errors will always be generated with conventional arithmetic if the output digits are changed, because each number has a unique representation.

### 3.3 Expectation of Overclocking Error

For a given  $T_S$ , the expectation of overclocking error can be obtained by combining  $Pr(T_S)$  from Algorithm 2 and  $|\varepsilon|$  from (11), as presented in (12). We first verify the proposed model against the results from Monte-Carlo simulations based on the aforementioned assumptions on timing and inputs, as shown in Figure 4(a) and Figure 4(b).  $T_S$  is normalized with respect to the value from structural timing analysis, i.e.  $(N + \delta)\mu$ . It can be seen that the modeled value match well with the simulation results. We also verify the models against the FPGA results without timing assumptions, as illustrated in Figure 4(c) and Figure 4(d). We notice that the general behavior of the model is similar to the FPGA implementation, however it does not capture the small increments in errors because we only model the coarse delay which is in units of  $\mu$ . Whereas the other sources of delay, such as the generation of the online inputs and result digits, are not modeled.

$$E_{ovc} = Pr(T_S) \cdot |\varepsilon| \quad (12)$$

From Algorithm 2, instead of accumulating  $Pr(T_S)$ , the probability of each individual chain delay  $Pr(d)$  are shown

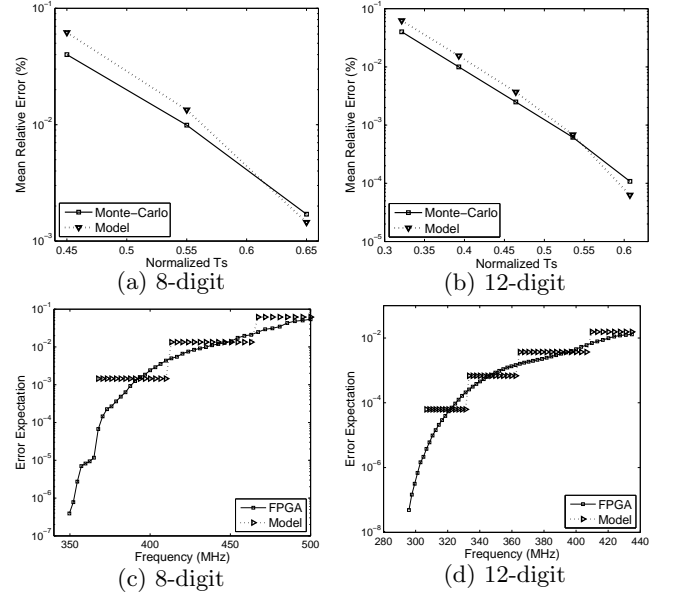


**Figure 4: Expectation of overclocking error for on-line multipliers: verification of the proposed model against Monte-Carlo simulations with timing assumptions (top row) and FPGA results with real timing information (bottom row).**

in Figure 5, together with the corresponding error magnitude  $|\varepsilon(d)|$  and the product of both  $E(d)$ , where parameter  $d$  represents the chain delay. For a given  $T_S$ , the overall error expectation in (12) can also be obtained from (13).

$$E_{ovc} = \sum_{d>b} Pr(d) \cdot |\varepsilon(d)| = \sum_{d>b} E(d) \quad (13)$$

From Figure 5 several observations can be made. First, the error magnitude decreases exponentially with longer chain lengths, because timing violation firstly affects LSDs with online arithmetic. Second, interestingly we see that carry chains with longer delay would happen with greater probabilities in an OM. This is because for the unrolled radix-2 OM,  $d(\tau)$  is only dependent upon the inputs for chain generation. Thus long chain will be generated as long as both input digits are not zeros with the probability of 4/9. Compared to the traditional arithmetic, carry generation, propagation and annihilation are all decided by specific input patterns. This limits the overall probability of long chains. However, we also notice that for chains with long delays, the increasing in likelihood of error is outweighed by the decrease in magnitude of error. Therefore the combination of both results in a decline in error expectation. In contrast, one would expect error expectation to grow faster as the amount of overclocking is increased when using traditional arithmetic because errors occur in MSBs.

## 4. CASE STUDY: IMAGE FILTER

### 4.1 Experimental Setup

The benefits of the proposed methodology are demonstrated by using a  $3 \times 3$  Gaussian image filter, which contains 9 multipliers and 8 adders, with two types of computer arithmetic. One is the radix-2 traditional arithmetic with data represented using 2's complement form. In this case, speed-optimized adders and multipliers are created using Xilinx

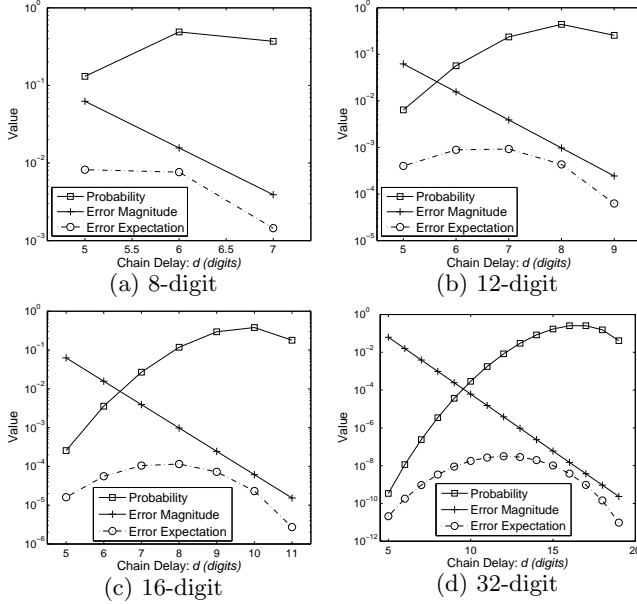


**Figure 5: Probabilities of different chain delay, the corresponding magnitude of overclocking error and the combination of both in terms of error expectation in a radix-2 OM.**

Core Generator [15]. The other is the radix-2 online arithmetic, with the basic building blocks as described in Section 2.2 and Section 2.3. In this case, all inputs and outputs are represented in the online format. In order to achieve the desired latency between input and output, both designs are overclocked and the errors seen at the output are recorded. The results are obtained from a Xilinx Virtex-6 FPGA through post place-and-route simulations. The results are evaluated in terms of mean relative error (MRE), which represents the percentage of error at outputs, as given by (14) where  $E_{error}$  and  $E_{out}$  refer to the mean value of error and correct output, respectively.

$$MRE = \left| \frac{E_{error}}{E_{out}} \right| \times 100\% \quad (14)$$

In our experiments, two types of input data are utilized. One is randomly sampled from a uniform distribution of  $N$ -digit numbers. This type is referred to as “Uniform Independent (UI) inputs”. The other is called “real inputs”, which are the pixel values of several  $512 \times 512$  benchmark images.

## 4.2 Quantify the Impact of Overclocking

The MRE values of the image filter with traditional arithmetic (dotted lines) and online arithmetic (solid lines) when  $N = 8$  are illustrated in Figure 6. According to the timing analysis tool, the rated operating frequencies of the two designs are 168.7MHz and 148.3MHz, respectively. However as seen in Figure 6, for the UI inputs, design with online arithmetic actually operates at a higher frequency without timing violations in comparison to the design using traditional arithmetic. This error-free frequency is even larger when using the real image data as inputs, since the real data do not exactly follow the uniform distribution or the independent assumption. In Figure 6 the “Lena” benchmark image is used as the real inputs.

If errors can be tolerated, we may allow timing violations to

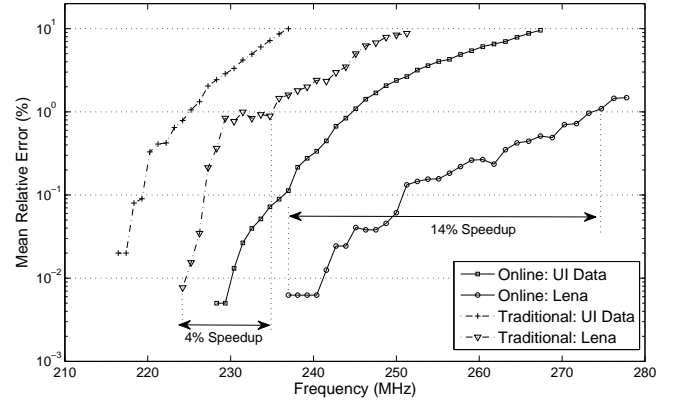


**Figure 6: Overclocking error in an image filter with two types of computer arithmetic: online arithmetic and standard binary arithmetic, of which the rated frequencies are 148.3MHz and 168.7MHz, respectively, according to the timing analysis tool.**

happen for better performance. The sensitivity of overclocking for a given arithmetic can be evaluated by the data slope in Figure 6. For instance under an error budget of 1% MRE, using UI inputs the frequency speedup of the traditional design is 3.89% with respect to the maximum frequency without errors, whereas the design with online arithmetic can be overclocked by 6.85%. This indicates that online arithmetic is less sensitive to overclocking, as discussed in Section 3.3. The difference is greater using real image data: 13.74% frequency speedup with online arithmetic against 4.04% with traditional arithmetic, because longer chains happen with a smaller probability with real inputs.

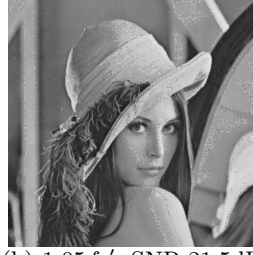
The output images for both design scenarios are presented in Figure 7. Since the overclocking errors are in the LSDs of the results with online arithmetic, the degradation on the image can be hardly observed. In contrast, timing violations cause error in the MSDs with traditional arithmetic. This leads to severe quality loss as shown on the images in the right column of Figure 7. Meanwhile, errors in the MSDs result in large noise power and therefore the signal-to-noise ratio (SNR) of the traditional design is small.

We also perform experiments using other benchmark images. The results are summarized in Table 1 and Table 2 in terms of the relative reduction of MRE and the improvements of SNR, respectively. In both tables the frequency is normalized to the maximum error-free frequency for each arithmetic. From Table 1, a significant reduction of MRE can be observed using online arithmetic. The geometric mean reduction of MRE is 89.2% using UI data. Even larger reductions of MRE can be achieved when testing with real image data, varying from 97.3% to 98.2%, as expected given the results shown in Figure 6. Similarly from Table 2, the improvements in SNR are 21.4dB ~ 43.9dB.

The area comparison between two designs is illustrated in Table 3. While we notice that our approach comes at some increase in area, the FPGA architecture is optimized for conventional arithmetic. For instance, the Virtex series employs dedicated multiplexers and encoders for very fast ripple carry addition [14]. Besides, at least 2 orders of magnitude error reduction is obtained for a given frequency in our design, as shown in Figure 6. Although the differences in



(a)  $1.05f_0$ , SNR=38.3dB



(b)  $1.05f_0'$ , SNR:21.5dB



(c)  $1.15f_0$ , SNR:36.2dB



(d)  $1.15f_0'$ , SNR:9.0dB



(e)  $1.25f_0$ , SNR:26.7dB



(f)  $1.25f_0'$ , SNR:8.5dB

**Figure 7: Output images of image filter using online arithmetic (left column) and traditional arithmetic (right column), where  $f_0$  and  $f_0'$  denote the maximum error-free frequencies for each design.**

both error and area can be compensated by using more digits with traditional arithmetic, this will result in longer delay and an even larger gap in frequency between two designs.

**Table 1: Relative Reduction of MRE with Online Arithmetic for Various Normalized Frequencies.**

Inputs	Normalized Frequency					Geo. Mean
	1.05	1.10	1.15	1.20	1.25	
Uniform	94.5%	89.1%	90.1%	88.3%	84.3%	89.2%
Lena	99.3%	99.2%	98.9%	97.7%	94.9%	97.9%
Pepper	99.7%	98.3%	98.1%	97.2%	95.1%	97.7%
Sailboat	99.5%	97.9%	97.3%	96.8%	95.1%	97.3%
Tiffany	99.9%	97.6%	98.4%	97.8%	97.2%	98.2%

## 5. CONCLUSION

In this paper, we have studied the probabilistic behavior of key arithmetic primitives with different computer arithmetic when operating beyond the deterministic region. Through the usage of analytical models and empirical FPGA results, we have demonstrated that significant error reduction and performance improvement can be achieved by using the “overclocking friendly” online arithmetic.

## 6. REFERENCES

- [1] T. Austin, D. Blaauw, T. Mudge, and K. Flautner. Making typical silicon matter with razor. *IEEE Trans.*

**Table 2: Improvement of SNR (dB) with Online Arithmetic for Various Normalized Frequencies.**

Inputs	Normalized Frequency				
	1.05	1.10	1.15	1.20	1.25
Lena	44.6	36.3	33.2	29.1	22.9
Pepper	35.7	28.3	28.7	25.9	24.1
Sailboat	33.7	27.5	26.3	25.0	21.7
Tiffany	43.9	25.9	29.5	25.6	24.5

**Table 3: FPGA Resource Usage Comparison.**

Metric	Arithmetic Type		Overhead
	Traditional	Online	
Look-Up Tables	912	1896	2.08
Slices	324	525	1.62

on Computer, 37(3):57–65, 2004.

- [2] A. Avizienis. Signed-digit number representations for fast parallel arithmetic. *IRE Trans. on Electronic Computers*, EC-10(3):389–400, 1961.
- [3] M. Ercegovac and T. Lang. On-the-fly conversion of redundant into conventional representations. *IEEE Trans. on Computer*, C-36(7):895–897, 1987.
- [4] M. D. Ercegovac. On-line arithmetic: An overview. In *Proc. Annual Technical Symp. Real time signal processing VII*, pages 86–93, 1984.
- [5] M. D. Ercegovac and T. Lang. *Digital arithmetic*. Morgan Kaufmann, 2003.
- [6] R. Galli and A. Tenca. A design methodology for networks of online modules and its application to the levinson-durbin algorithm. *IEEE Trans. on VLSI*, 12(1):52–66, 2004.
- [7] V. Gupta, D. Mohapatra, A. Raghunathan, and K. Roy. Low-power digital signal processing using approximate adders. *IEEE Trans. on CAD of Integrated Circuits and Systems*, 32(1):124–137, 2013.
- [8] Y. Harata, Y. Nakamura, H. Nagase, M. Takigawa, and N. Takagi. A high-speed multiplier using a redundant binary adder tree. *IEEE Jounl. of Solid-State Circuits*, 22(1):28–34, 1987.
- [9] Z. M. Kedem, V. J. Mooney, K. K. Muntimadugu, and K. V. Palem. An approach to energy-error tradeoffs in approximate ripple carry adders. In *Proc. Int. Symp. on Low Power Elec. and Design*, pages 211–216, 2011.
- [10] P. Kulkarni, P. Gupta, and M. Ercegovac. Trading accuracy for power with an underdesigned multiplier architecture. In *Proc. Int. Conf. on VLSI Design*, pages 346–351, 2011.
- [11] S. Rajagopal and J. Cavallaro. Truncated online arithmetic with applications to communication systems. *IEEE Trans. on Computers*, 55(10):1240–1252, 2006.
- [12] N. Takagi, H. Yasuura, and S. Yajima. High-speed VLSI multiplication algorithm with a redundant binary addition tree. *IEEE Trans. on Computers*, 100(9):789–796, 1985.
- [13] K. S. Trivedi and M. Ercegovac. On-line algorithms for division and multiplication. *IEEE Trans. on Computers*, 26:161–167, 1975.
- [14] Xilinx. Virtex-6 FPGA configurable logic block user guide.
- [15] Xilinx. LogiCORE IP multiplier v11.2, 2011.